Critical exponents of the $La_{0.7}Sr_{0.3}MnO_3$, $La_{0.7}Ca_{0.3}MnO_3$, and $Pr_{0.7}Ca_{0.3}MnO_3$ systems showing correlation between transport and magnetic properties

Subhrangsu Taran and B. K. Chaudhuri
Solid State Physics Department, Indian Association for the Cultivation of Science, Jadavpur, Kolkata-700032, India

Sandip Chatterjee[a)]
Department of Physics, Government College of Engineering and Textile Technology, Serampore-712201, West Bengal, India

H. D. Yang
Department of Physics, National Sun Yat Sen University, Kaohsiung, Taiwan, Republic of China

S. Neeleshwar and Y. Y. Chen
Institute of Physics, Academia Sinica, Taipei, Taiwan, Republic of China

(Received 29 April 2005; accepted 11 September 2005; published online 18 November 2005)

From the low-temperature (down to 10 K) dc-magnetization data of the $La_{0.7}Sr_{0.3}MnO_3$ (LSM), $La_{0.7}Ca_{0.3}MnO_3$ (LCM), and $Pr_{0.7}Ca_{0.3}MnO_3$ (PCM) systems, we estimated the critical exponents β, γ, and hence δ from the analysis of the modified Arrot plots. The exponent β estimated for the LCM system is less than that predicted by Heisenberg model and resides within the zone predicted by Ising model while for the LSM sample, β is higher than that predicted from the Heisenberg model which is considered to be due to the presence of dipole-dipole interaction arising from the large spin moment in the LSM system. The magnetization data of the PCM system cannot be fitted to the modified Arrot plots, which suggest highly inhomogeneous ground state even under 5 T magnetic field. Both LSM and LCM have almost equal values of γ. Seebeck coefficient data indicate a crossover from higher-temperature *n*-type to lower-temperature *p*-type conductivity behavior in both LSM and LCM systems, while the semiconducting PCM system shows *p*-type conductivity throughout the temperature range (300–80 K). It is noticed that for LSM system T_C (Curie temperature) and T_{MI} (metal-insulator transition temperature) are almost equal ($\sim$360 K), whereas for the LCM system there exist a large difference between T_C and T_{MI} ($T_C \sim 245$ K and $T_{MI} \sim 265$ K), which may give some idea regarding the critical behavior of the respective samples. [DOI: 10.1063/1.2128467]

I. INTRODUCTION

In recent years elaborate structural and other properties of $R_{1-x}M_xMnO_3$- (R=rare-earth elements and M=divalent metal such as Ca, Sr, Ba, etc.) type perovskite materials have been made[1] to understand the mechanism of transport and spin ordering in them. Substitution for trivalent R^{3+} with divalent M^{2+} ions produces holes, which are mobile via hybridized orbital of Mn $3d$-e_g and O $2p$-σ and mediate the ferromagnetic (FM) double-exchange (DE) interaction between localized Mn spins in the t_{2g} states.[2–4] The change in the valence of the perovskite *A*-site or the band filling, significantly affects the magnetism and conductivity of these manganites.[5,6] Recent investigations have demonstrated that variations in *A*-site ions play important roles in the magnetic and transport properties of these manganites for a given carrier doping.[7,8] A direct relationship between the average ionic radius for *A*-site ions $\langle r_A \rangle$ and the Curie temperature T_C has already been established.[9]

Among various manganites with perovskite structure, $La_{0.7}Sr_{0.3}MnO_3$ (LSM) is a prototype DE ferromagnet and it is mostly metallic and therefore has most itinerant electrons. Replacement of Sr by Ca results in a distortion of MnO_6 octahedra (hence increase of electron-phonon coupling), which lowers T_C with increase of resistivity of the $La_{0.7}Ca_{0.3}MnO_3$ (LCM) system. Moreover, the $Pr_{1-x}Ca_xMnO_3$ (PCM) is perhaps the most interesting because of its ordered phases which are very sensitive to doping.[10–17] It is well known that the T_C values of the $AMnO_3$-type manganites can be continuously varied by suitable substitutions. When the doping at the *A* site with bivalent ions is kept constant, the main effect of the *A*-site substitutions is to change the structural parameters such as Mn–O–Mn bond angle and Mn–O bond lengths, allowing the study of the effect of structure change on the magnetic and other properties.

Like distinguishing transport and magnetic behaviors of the LSM-, LCM-, and PCM-type systems, their critical exponents are also distinctive and even sensitive to the doping effect providing interesting information about the magnetic spin ordering behavior in these materials. Although, several groups have already reported magnetic and transport proper-

[a)]Author to whom correspondence should be addressed; electronic mail: sndp_chtt@yahoo.com

ties of LSM, LCM, and PCM systems, very few studies have been made on the critical behavior. Moreover, the critical exponents obtained from magnetic and other studies are inconsistent which vary fairly widely. Critical exponents of the manganite system are important parameters. One can expect some correlations between the variation of the transport property of the sample with the corresponding fluctuation of the critical exponents.

In this paper, we have presented magnetic (magnetization) behavior of three manganite systems, viz., LSM, LCM, and PCM. From the analysis of dc-magnetization data (down to 10 K), the critical exponents β and γ (hence δ) have been calculated by using modified Arrot plots. It is shown that the critical exponents of the similar manganite systems vary depending on the ground-state behavior of the samples. This is also well reflected from the resistivity and thermoelectric power (which is additive in nature and does not depend on grain boundary) data of these perovskite compounds.

II. EXPERIMENT

The samples of the present study were prepared by mixing stoichiometric quantities of La_2O_3, $SrCO_3$, $CaCO_3$, Pr_6O_{11}, and $Mn(CH_3COO)_2 \cdot 4H_2O$ and were preheated at 600 °C. The resulting powder was repeatedly grinded and annealed at 1200 °C and at final stage it was pelletized and annealed at 1250 °C in air for 24 h and furnace cooled at a steady rate of 5 °C/min to make a dense sample. The single-phase character of all the samples was confirmed by X-ray diffraction (XRD) study with Cu $K\alpha$ radiation.

Resistivity of the samples was measured by a conventional four-probe method.[7] The bulk samples were cut into definite rectangular shape and the electrical connections were made by good quality silver paint. Data have been taken for both forward and reversed current directions to minimize offset voltage and thermal effect. Thermoelectric power was measured by using steady-state method.[18] A resistive heater connected at one end of the sample generated a thermal gradient between the two ends of the sample. The gradient was measured by a copper-constantan thermocouple. The temperature of the sample was measured by a *K*-type thermocouple within the temperature range of 80–300 K. The magnetization data were collected using a commercial (Quantum Design Inc.) superconducting quantum interference device (SQUID) magnetometer.

III. RESULTS AND DISCUSSIONS

Magnetic field and temperature dependent magnetization (M) and susceptibility (χ) of all the three samples are shown in Figs. 1 and 2, respectively. Experimental data presented in Fig. 2 have been taken around the FM to paramagnetic (PM) transition temperature. These results are in good agreement with those reported earlier.[19,20] It is found from Fig. 2 that the magnetization M for LSM and LCM saturates in the FM state, while for PCM, M does not saturate even under the magnetic field of 5 T. This happens due to the presence of charge-ordered antiferromagnetic (CO-AFM) state in the PCM system. Ferromagnetic Curie temperature T_C is estimated from Fig. 1. The FM behavior around T_C can be studied with the M^2 vs H/M plots (namely, Arrot plot).[21,22] The straight-line nature of the M^2 vs H/M curves intercepts the H/M axis, and determines the magnetic state (negative below T_C and positive above T_C). The mean-field approximation can be generalized to the so-called modified Arrot expression[23]

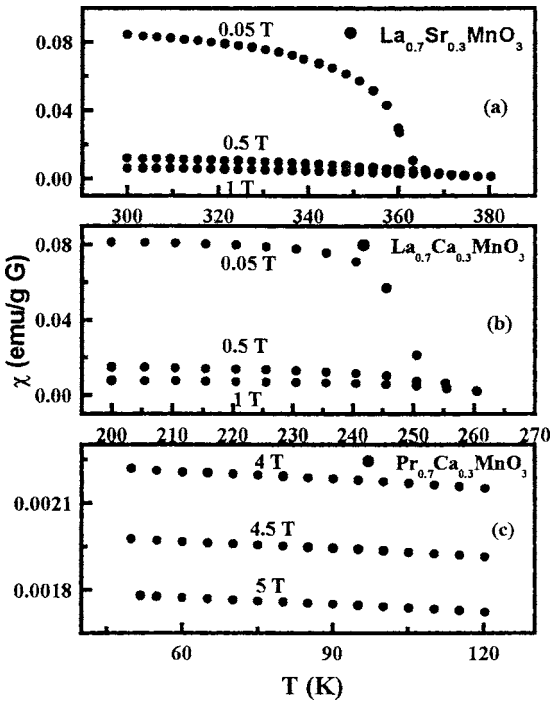

FIG. 1. Susceptibility (χ) of (a) $La_{0.7}Sr_{0.3}MnO_3$, (b) $La_{0.7}Ca_{0.3}MnO_3$, and (c) $Pr_{0.7}Ca_{0.3}MnO_3$ as a function of temperature at different magnetic fields.

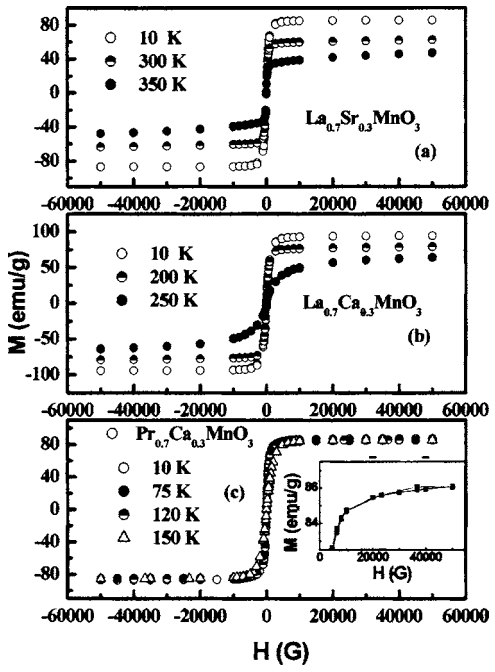

FIG. 2. Magnetization (M) of (a) $La_{0.7}Sr_{0.3}MnO_3$, (b) $La_{0.7}Ca_{0.3}MnO_3$, and (c) $Pr_{0.7}Ca_{0.3}MnO_3$ as a function of magnetic field at different temperatures. Inset of (c) shows the increase of magnetization with increase of magnetic field (i.e., magnetization value is not saturating even with the application of 5 T magnetic field).

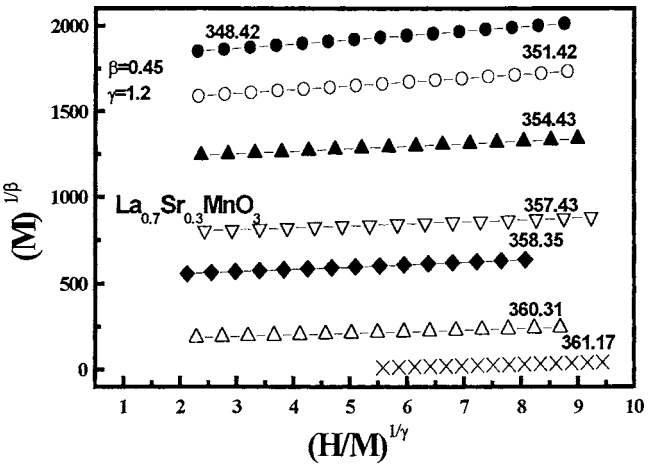

FIG. 3. Modified Arrot plot to calculate the critical exponents [β and γ by iteration process from Eq. (1)] for the $La_{0.7}Sr_{0.3}MnO_3$ systems. Isothermal curves fall into a set of parallel straight lines when the proper values of the exponents are chosen.

$$(H/M)^{1/\gamma} = C_1(T - T_C) + C_2 M^{1/\beta}, \tag{1}$$

which combines the relations for the spontaneous magnetization below T_C

$$M \sim (T_C - T),$$

and the inverse magnetic susceptibility above T_C

$$\chi^{-1} \sim (T - T_C).$$

To find the correct values of β and γ, an initial choice of β and γ is taken, yielding quasistraight lines in the modified Arrot plot. From these initial values of β and γ, linear fits to the isotherms are made to get the intercepts giving $M(T)$ and $\chi(T)$. These new values of β and γ are then used to make a new modified Arrot plot. New values for the critical exponents thus obtained are reintroduced in the scaling of the modified Arrot plot. The process is repeated until the iteration converges, leading to an optimum fitting value. Figure 3 shows the final results for LSM of these iterations. The isotherms are quite parallel with slopes very close to each other. The final values of β and γ for LSM samples are 0.45 and 1.2, respectively, whereas for LCM sample (Fig. 4) the values are, respectively, 0.36 and 1.2. The estimated value of β for LSM, therefore, resides between mean-field theory (β =0.50) and Heisenberg model (β=0.37) and γ value (=1.2) lies near the Ising model (γ=1.24). For LCM sample, the value of β(=0.36) lies in between the Heisenberg and Ising models (β=0.33) whereas the value of γ(1.2) is also near the theoretical Ising value (1.24).

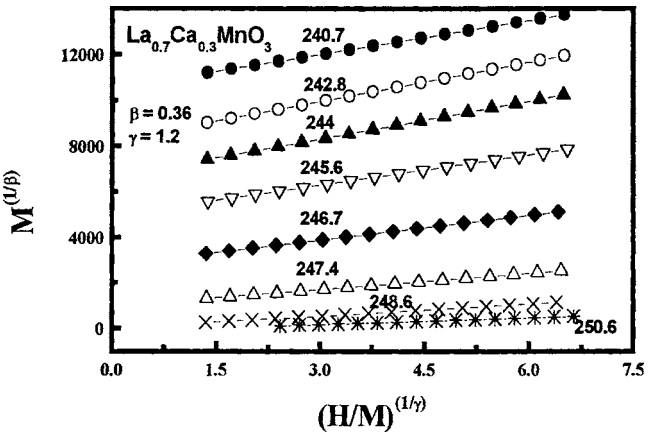

FIG. 4. Modified Arrot plot to calculate the critical exponents [β and γ by iteration process from Eq. (1)] for the $La_{0.7}Ca_{0.3}MnO_3$ system.

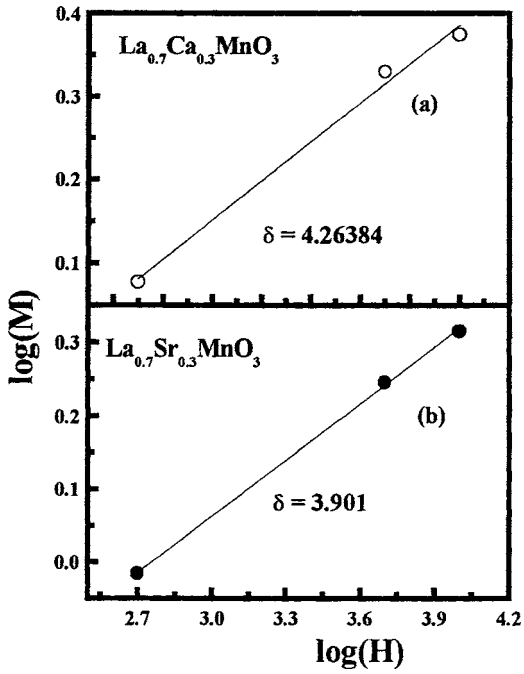

FIG. 5. Plot of $\log(M)$ vs $\log(H)$ at Curie temperature (T_C) to calculate the critical exponent (δ) for the systems (a) $La_{0.7}Sr_{0.3}MnO_3$ and (b) $La_{0.7}Ca_{0.3}MnO_3$ shown in Table I.

Figure 5 shows $\ln(M)$ vs $\ln(H)$ plot (using the critical isotherm) for both LSM and LCM samples, the inverse of which is used to determine the value of the critical exponent δ. The obtained values of δ for LSM and LCM samples are, respectively, 3.901 and 4.263. The values match well with those (δ=3.666 and 4.333) determined by using the Widen scaling equation $\delta = 1 + \gamma/\beta$. Table I shows the values of the exponents estimated by different groups for comparison with those of our estimated values. In the case of LSM the critical exponents as found from magnetic measurements (this work) are consistent with those observed by Ziese.[24] This is also consistent with the finding of a recent investigation of the double-exchange mechanism using Monte Carlo simulations, which indicates that the values of critical exponents are nearer to those of Heisenberg model.[25] Fisher *et al.*[26] showed that the critical exponents approach the value of the Heisenberg model if the exchange interaction has the form $J(r) \sim r^{-d-\nu}$ with $2\nu > d$, whereas mean-field values are found for $2\nu < d$. Here d is the spatial dimension. Since the magnetic interaction is mediated by the double-exchange interaction and is supposed to be short range, even at low temperatures typical mean free paths do not exceed one to two lattice spacing.[27] Therefore, critical behavior in LSM, consistent with the Heisenberg model is expected.

Gehring and Coombes[28] found that a Mn-ion triplets containing one hole, i.e., a Mn^{3+}–Mn^{4+}–Mn^{3+} cluster has a

TABLE I. Critical exponents for manganite systems as determined by various methods, viz., bulk magnetization measurements $M(H)$, ferromagnetic antiresonance FMAR, n scattering (neutron scattering), and μ^+ spin resonance μSR.

Compound	Method	T_C (K)	β	γ	Reference
$La_{0.7}Sr_{0.3}MnO_3$	$M(H)$	360.6	0.45±0.02	1.08±0.04	24
$La_{0.7}Sr_{0.3}MnO_3$	FMAR	361	0.45	[a]	33
$La_{0.7}Sr_{0.3}MnO_3$	n scattering	350.8	0.30±0.02	[a]	34
$La_{0.7}Sr_{0.3}MnO_3$	$M(H)$	357	0.45±0.01	1.2	This study
$La_{0.67}Ca_{0.33}MnO_3$	μSR	274.3	0.345±0.015	[a]	20
$La_{0.7}Ca_{0.3}MnO_3$	$M(H)$	248	0.36±0.01	1.2	This study
$La_{0.75}Sr_{0.25}MnO_3$	$M(H)$	346	0.40±0.02	1.27±0.06	35

[a]Not available.

significant binding energy of about half the binding energy of the bulk. These large spin moments enhance the dipole-dipole interaction in the case of Heisenberg model. As shown in Table I, the obtained β value in the LSM sample is higher than that expected in the Heisenberg model. This might be due to the above mentioned dipole-dipole interactions. It is to be mentioned that in LSM sample, γ is more closer to that of Ising model. Our estimated γ value is consistent with that reported by Ghosh *et al.*[29]

The critical exponents measured from our present work indicate that the magnetic order in LCM is of short-range character. This is due to the fact that the ground state of LCM is inhomogeneous. Moreover, the magnetization data cannot be fitted with Eq. (1) for the PCM system even under high magnetic field (5 T). This also indicates that the ground state inhomogeneity is much more in the PCM sample which makes it semiconducting without showing metal-insulator transition.

The inhomogeneous character of the ground state and different critical behavior of the LSM, LCM, and PCM are also reflected in their resistivity and thermoelectric power data shown in Figs. 6 and 7 for comparison. LSM has MI transition around 350 K. LCM undergoes a metal-insulator (MI) transition around 265 K. The decrease of $\rho(T)$ value under the application of magnetic field of 1.2 T is higher in LCM than that observed in LSM. The temperature variation of resistivity of PCM shows the insulating behavior down to the lowest temperature of measurement (15 K).

The TEP (S), which is regarded as the volume average measurement show similar behavior for both LCM and LSM (Fig. 7) and consistent with those reported earlier.[30,31] The behavior of $S(T)$ for the LCM sample is similar to that of LSM but the value is more negative compared with that of LSM. Moreover, the maximum observed around 140 K for LCM sample is lower than that of LSM. For the LCM an anomaly is also observed around the MI transition temperature. TEP value of PCM system is large and has an insulatorlike behavior with $1/T$. The observed behavior of S is consistent with the resistivity data of these samples. However, above ~140 K (in the case of LCM) and ~170 K (for LSM) the value of TEP decreases with increasing temperature. It changes sign at around 225 and 275 K for LCM and LSM, respectively. Near the transition temperature, none of the manganites, LCM or LSM, exhibit any maxima in S versus temperature curve. These features can be treated as an indication of the electron contribution to the S. The electron contribution to the TEP appears not far from the upper boundary of the metallic state and, therefore, can be related with the process of localization. This is supported from the fact that in LCM, in which the upper boundary of the metallic state is ~200 K, the maxima of S lies at 140 K. While in LSM, in which the metallic state ranges up to ~225 K, S is maximum at 170 K.

More distinguishing behavior of TEP values of LSM and LCM is obtained from the S vs ρ plots (Fig. 8). It is found that for LSM, below metal-insulator transition temperature (T_{MI}) (i.e., in FM metallic region), S increases with increase of ρ but above T_{MI}, S decreases with the increase of ρ. Below T_{MI}, the rate of increase enhances abruptly above a certain ρ

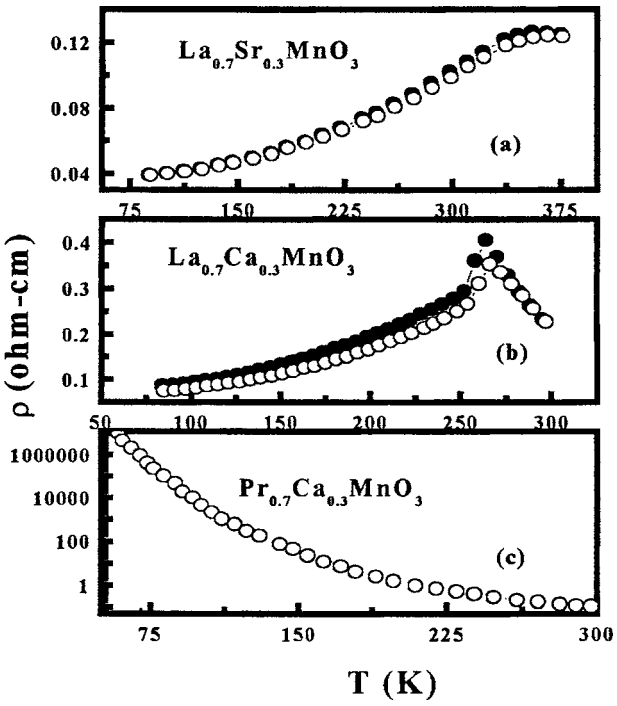

FIG. 6. The temperature variation resistivity of (a) $La_{0.7}Sr_{0.3}MnO_3$ and (b) $La_{0.7}Ca_{0.3}MnO_3$ in presence (H=1.2 T) and in absence of magnetic field (H), and that of (c) $Pr_{0.7}Ca_{0.3}MnO_3$ in zero field showing no metal-insulator transition for the system which is a CO-AFM.

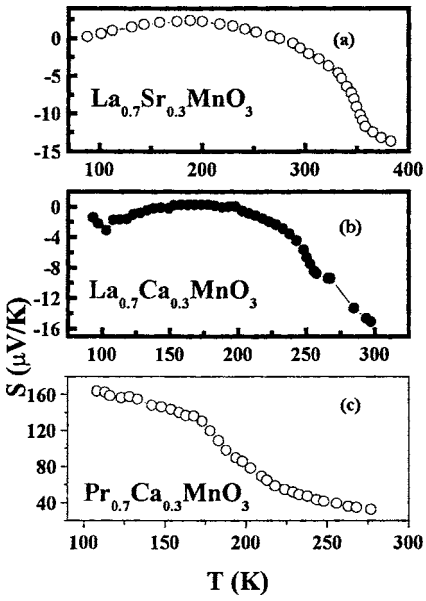

FIG. 7. The temperature variation thermoelectric power (Seebeck coefficient) of (a) $La_{0.7}Sr_{0.3}MnO_3$, (b) $La_{0.7}Ca_{0.3}MnO_3$, and (c) $Pr_{0.7}Ca_{0.3}MnO_3$.

value. In the case of LCM sample, below T_{MI}, S increases with ρ monotonically. Moreover, above T_{MI}, S increases with the increase of ρ.

In general, the feature of diffusion thermopower can be qualitatively understood in terms of Mott's formula for the charge contribution in metals to the Seebeck coefficient in metals.[32]

$$S = \Pi^2/3(k_B^2 T/e)\sigma'(E_F)/\sigma(E_F), \tag{2}$$

where e is the elementary charge, $\sigma(E_F)$ is the conductivity at Fermi, and $\sigma'(E_F)$ stands for $d[\sigma(E_F)]/dE$. If σ is assumed constant and almost isotropic electrical transport properties, i.e., $\sigma^{-1}=\rho$, then according to Eq. (2), S should be proportional to ρ. For the LSM sample in ferromagnetic metallic (FMM) region, it is obvious that S vs ρ behavior cannot be explained properly if σ' is assumed to be a constant. This deviation might be associated with other contribution such as phonon-drag effect. For LCM, below T_{MI}, σ is found to be constant and one might conclude from the above discussion that in LSM sample phonon-drag effect might be a possibility, whereas in LCM it is absent. This could be, as discussed earlier, due to the fact that in LSM T_C is high and the ground state is homogeneous, whereas in LCM T_C is lower and the corresponding ground state is inhomogeneous. Above T_{MI}, S vs ρ behavior (Fig. 8) in LSM is opposite to that in LCM sample. The observed differences in the S vs ρ curves in LSM and LCM are related to the differences in their critical behavior. Therefore, one can predict that for Heisenberg system (as in LSM), T_C and T_{MI} are almost equal, whereas for the system which deviates from Heisenberg to Ising type, the T_C and T_{MI} differs appreciably. Moreover, as the system is changing from Heisenberg to Ising-model-type behavior, the value of TEP tends to become more negative.

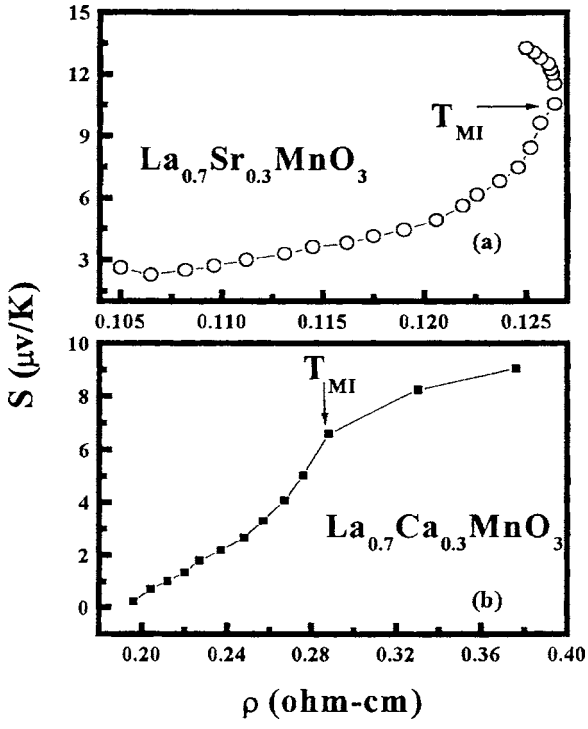

FIG. 8. Thermoelectric power vs resistivity plot for the systems (a) $La_{0.7}Sr_{0.3}MnO_3$ (LSM) and (b) $La_{0.7}Ca_{0.3}MnO_3$ (LCM) showing the different behavior of the two metallic systems which reflects in the critical behavior (exponents) of these system (Table I).

IV. CONCLUSION

Low-temperature resitivity and thermoelectric power of both the LSM and LCM systems indicate activated carrier transport in the high-temperature phase ($T>T_C$) and metallic-like transport behavior below T_C, but only activated carrier transport mechanism for the PCM system throughout the temperature range of present investigation. Estimated critical exponents (β, γ, and hence δ) from low-temperature magnetic measurements of three CMR samples LSM, LCM, and PCM show significant sample dependent behavior. From a comparative study of the transport (resistivity and Seebeck coefficients) and magnetic properties of LSM, LCM, and PCM, a fair correlation between the magnetic and transport behaviors has been observed. The obtained value of the exponent β in LSM is higher than that expected from the Heisenberg model, which might be due to the presence of dipole-dipole interaction. In LCM sample, the critical exponent indicates that the magnetic ordering is of short range. This is considered to be due to the fact that the ground state of LCM is inhomogeneous. In the case of PCM no value of critical constant is observed from magnetization data even under the application of high magnetic field. This is considered to be due to the fact that in this sample the ground state is highly inhomogeneous. Like critical exponents estimated from the low-temperature magnetization data, the thermoelectric power and resistivity data might also be used to provide interesting clues to the signature of magnetic character (Heisenberg or Ising-type behavior) of the LSM- and LCM-type samples.

ACKNOWLEDGMENT

The author (S.T.) is grateful to CSIR for the financial support.

[1]E. Dagotta *et al.*, Phys. Rep. **344**, 1 (2001).
[2]C. Zener, Phys. Rev. **81**, 440 (1951).
[3]P. W. Anderson and H. Hesegawa, Phys. Rev. **100**, 675 (1955).
[4]P. G. de Gennes, Phys. Rev. **118**, 141 (1960).
[5]E. O. Wollen and W. C. Kochler, Phys. Rev. **100**, 545 (1955).
[6]A. Urushibara, Y. Maritomo, T. Arima, A. Asamitsu, G. Kido, and Y. Tokura, Phys. Rev. B **51**, 14103 (1995).
[7]S. Taran, S. Chatterjee, and B. K. Chaudhuri, Phys. Rev. B **69**, 184413 (2004).
[8]S. Chatterjee and A. K. Nigam, Phys. Rev. B **66**, 104403 (2002).
[9]C. R. Mahendiran, R. Mahesh, A. K. Raychaudhuri, and C. N. R. Rao, Phys. Rev. B **53**, 12160 (1996).
[10]S.-Q. Shen and Z. D. Wang, Phys. Rev. B **61**, 9532 (2000).
[11]M. R. Lees, J. Barratt, G. Balakrishnan, D. M. Paul, and M. Yethiraj, Phys. Rev. B **52**, R14303 (1995).
[12]M. R. Lees, O. A. Petrenko, G. Balakrishnan, and D. Mck. Paul, Phys. Rev. B **59**, 1298 (1999).
[13]Y. Tomioka, A. Asamitsu, H. Kuwahara, Y. Moritomo, and Y. Tokura, Phys. Rev. B **53**, R1689 (1996).
[14]C. Martin, A. Maignan, M. Hervieu, and B. Raveau, Phys. Rev. B **60**, 12191 (1999).
[15]H. Yoshizawa, H. Kawano, Y. Tomioka, and Y. Tokura, Phys. Rev. B **52**, R13145 (1995).
[16]H. Yoshizawa, H. Kawano, Y. Tomioka, and Y. Tokura, J. Phys. Soc. Jpn. **65**, 1043 (1996).
[17]A. Anane, J. P. Renard, L. Reversat, C. Dupas, P. Veillet, M. Viret, L. Pinsard, and A. Revcolevschi, Phys. Rev. B **59**, 77 (1999).
[18]A. Banerjee, S. Pal, S. Bhattacharya, H. D. Yang, and B. K. Chaudhuri, Phys. Rev. B **64**, 104428 (2001).
[19]R. Mahendiran, R. Ramesh, A. K. Roychaudhuri, and C. N. R. Rao, Solid State Commun. **99**, 149 (1996).
[20]K. H. Kim, J. Y. Gu, H. S. Choi, G. W. Park, and T. W. Noh, Phys. Rev. Lett. **77**, 1877 (1996).
[21]A. Arrot, Phys. Rev. **108**, 1394 (1957).
[22]K. P. Bolov, *Magnetic Transitions* (Boston Technical, Boston, 1965).
[23]A. Arrot and J. E. Noakes, Phys. Rev. Lett. 19, 796 (1967).
[24]M. Ziese, J. Phys.: Condens. Matter **13**, 2919 (2001).
[25]J. Alonso, L. A. Fernanadez, F. Guinea, V. Laliena, and V. Martin-Mayor, cond-mat/0007450.
[26]M. E. Fisher, S.-K. Ma, and B. G. Nickel, Phys. Rev. Lett. **29**, 917 (1972).
[27]M. Ziese and C. Srinitiwarawong, Phys. Rev. B **58**, 11519 (1998).
[28]G. A. Gehring and D. J. Coombes, J. Magn. Magn. Mater. **873**, 177 (1998).
[29]K. Ghosh, C. J. Lobb, R. L. Greene, S. G. Karabashev, D. A. Shulyatev, A. A. Arsenov, and Y. Mukovskii, Phys. Rev. Lett. **81**, 4740 (1998).
[30]N. G. Bebenin, R. I. Zainullina, V. V. Mashkautsan, V. V. Ustinov Ya, and M. Mukovskii, Phys. Rev. B **69**, 104434 (2004).
[31]A. Asamitsu, Y. Moritomo, and Y. Tokura, Phys. Rev. B **53**, R2952 (1996).
[32]M. Cutler and N. F. Mott, Phys. Rev. **181**, 1336 (1969).
[33]S. E. Lofland, V. Ray, P. H. Kim, S. M. Bhagat, M. A. Manheimer, and S. D. Tyagi, Phys. Rev. B **55**, 2749 (1997).
[34]L. Vasilìu-Doloc, J. W. Lynn, Y. M. Mukovskii, A. A. Arsenov, and D. A. Shulyatev, J. Appl. Phys. **83**, 7342 (1998).
[35]D. Kim, B. L. Zink, F. Hellman, and J. M. D. Coey, Phys. Rev. B **65**, 214424 (2002).